Laser Scanning Up-Conversion Luminescence Microscopy for Imaging Cells Labeled with Rare-Earth Nanophosphors. Anal Chem

ARTICLE *in* ANALYTICAL CHEMISTRY · FEBRUARY 2009

Impact Factor: 5.64 · DOI: 10.1021/ac802072d · Source: PubMed

Anal. Chem. **2009,** *81,* 930–935

Laser Scanning Up-Conversion Luminescence Microscopy for Imaging Cells Labeled with Rare-Earth Nanophosphors

Mengxiao Yu,[†] Fuyou Li,*[,†] Zhigang Chen,[†] He Hu,[†] Cheng Zhan,[‡] Hong Yang,[†] and Chunhui Huang[†]

Department of Chemistry and Laboratory of Advanced Materials, Fudan University, Shanghai, 200433, P. R. China, and National Institute of Biological Science, Beijing, 102206, P. R. China

Because of the ability to selectively reveal the objects of interest with subcellular resolution, fluorescence microscopy provides widespread applications from basic biological research to clinical diagnosis. However, challenges still remain in reducing the degree of photobleaching and increasing the contrast between signal and noise. Herein, we found that rare-earth nanophosphors exhibit a unique up-conversion luminescence mechanism and imaging modality and developed a new three-dimensional visualization method of laser scanning up-conversion luminescence microscopy (LSUCLM) with little photobleaching and no background fluorescence, by introducing a reverse excitation dichroic mirror and the confocal pinhole technique. Moreover, we demonstrated the up-conversion emission imaging of thin films containing embedded rare-earth nanophosphors and cells multilabeled with the nanophosphors and organic dyes. These data show that LSUCLM not only shares noninvasive benefits and deep penetration of two-photon microscopy but also offers some distinct advantages, such as little photobleaching of both organic dyes and rare-earth nanophosphors, no background fluorescence from either endogenous fluorophores or colabeled fluorescent probes, and excellent compatibility with conventional confocal microscopy.

Microscopy is a powerful tool for the manipulation and investigation of microspecies, such as biologic cells and inorganic colloids.[1−10] Particularly, fluorescence microscopy offers a unique approach for visualizing morphological details in tissue with subcellular resolution that cannot be resolved by ultrasound or magnetic resonance imaging.[1−6] Over the years, many of the improvements in fluorescence imaging have been focused on developing a novel fluorescence microscopy method and biological luminescent labels to increase the imaging depth, to reduce photobleaching, to enhance the contrast between what is interesting (signal) and what is not (background), and etc.

Conventional wide-field fluorescence microscopy yields poor image quality, because the in-focus detail is obscured greatly by out-of-focus fluorescence.[1] By virtue of a confocal pinhole to eliminate the background caused by out-of-focus light and scatter, laser scanning confocal microscopy improves spatial resolution within the focus plane and provides depth discrimination.[2,3] Nevertheless, confocal microscopy is still associated with some drawbacks, such as limited imaging depth (a few tens of micrometers), photodamage, and photobleaching,[1,3,6] owing to the use of short-wavelength (higher-energy) ultraviolet or visible light as the excitation source of conventional down-conversion luminescent labels (such as organic dyes,[11,12] fluorescent proteins,[13] metal complexes,[14] and semiconductor quantum dots[15]). The subsequent invention of two-photon microscopy greatly reduced these problems by using excitation with long-wavelength femtosecond pulses ($\sim 10^{-13}$ s).[4−6] The long-wavelength (low-energy) light penetrates deeper (hundreds of micrometers) into samples, while photodamage and photobleaching outside of the focal plane are reduced, and inherent three-dimensional resolution is obtained. As a result from the utilization of expensive femtosecond pulses (~$200 000),[5,6] unfortunately, two-photon microscopy also has some intrinsic limitations, such as accelerated photobleaching

* To whom correspondence should be addressed. Fax: 86-21-55664621. Phone: 86-21-55664185. E-mail: fyli@fudan.edu.cn.

[†] Fudan University.

[‡] National Institute of Biological Science.

(1) Stephens, D. J.; Allan, V. J. *Science* **2003**, *300*, 82–86.
(2) Matsumoto, B. *Methods in Cell Biology: Cell Biological Applications of Confocal Microscopy*, 2nd ed.; Academic Press: San Diego, CA, 2002; Vol. 70.
(3) Conchello, J. A.; Lichtman, J. W. *Nat. Methods* **2005**, *2*, 920–931.
(4) Cahalan, M. D.; Parker, I.; Wei, S. H.; Miller, M. *Nat. Rev. Immunol.* **2002**, *2*, 872–880.
(5) Zipfel, W. R.; Williams, R. M.; Webb, W. W. *Nat. Biotechnol.* **2003**, *21*, 1369–1377.
(6) Stutzmann, G. E.; Parker, I. *Physiology* **2005**, *20*, 15–21.
(7) Schuttpelz, M.; Muller, C.; Neuweiler, H.; Sauer, M. *Anal. Chem.* **2006**, *78*, 663–669.
(8) Xie, X. S.; Yu, J.; Yang, W. Y. *Science* **2006**, *312*, 228–230.
(9) Poggi, M. A.; Gadsby, E. D.; Bottomley, L. A.; King, W. P.; Oroudjev, E.; Hansma, H. *Anal. Chem.* **2004**, *76*, 3429–3444.
(10) Brucherseifer, M.; Kranz, C.; Mizaikoff, B. *Anal. Chem.* **2007**, *79*, 8803–8806.
(11) Haugland, R. P. *A Guide to Fluorescent Probes and Labelling Technologies*, 10th ed.; Molecular Probes: Eugene, OR, 2005; www.probes.com and www.invitrogen.com.
(12) Zhang, M.; Yu, M. X.; Li, F. Y.; Zhu, M. W.; Li, M. Y.; Gao, Y. H.; Li, L.; Liu, Z. Q.; Zhang, J. P.; Zhang, D. Q.; Yi, T.; Huang, C. H. *J. Am. Chem. Soc.* **2007**, *129*, 10322–10323.
(13) Giepmans, B. N. G.; Adams, S. R.; Ellisman, M. H.; Tsien, R. Y. *Science* **2006**, *312*, 217–224.
(14) Yu, M. X.; Zhao, Q.; Shi, L. X.; Li, F. Y.; Zhou, Z. G.; Yang, H.; Yi, T.; Huang, C. H. *Chem. Commun.* **2008**, 2115–2117.
(15) Michalet, X.; Pinaud, F. F.; Bentolila, L. A.; Tsay, J. M.; Doose, S.; Li, J. J.; Sundaresan, G.; Wu, A. M.; Gambhir, S. S.; Weiss, S. *Science* **2005**, *307*, 538–544.

10.1021/ac802072d CCC: $40.75
Published on Web 01/06/2009

within the focused volume and a limited number of investigators. In particular, owing to the similar luminescence processes of conversional luminescent labels and ubiquitous endogenous components in biological samples, background autofluorescence cannot be completely suppressed regardless of single-photon or two-photon relative excitation.[16−18] To solve these problems, it is necessary to develop a new microscopy method based on other photoluminescence processes and other luminescent labels.

As an alternative, novel microscopy may be exploited based on the up-conversion luminescence (UCL) of rare-earth up-converting nanophosphors (UCNPs). UCNPs exhibit excellent luminescence properties (such as sharp emission lines and long lifetimes) by a unique UCL process,[19−29] whereby continuous-wave (CW) low-energy light in the near-infrared region (such as 980 nm) is converted to higher-energy visible light through multiple photon absorption or energy transfer. It may reasonably be postulated that UCNPs would seem to be appealing targets for eliminating background fluorescence in biological applications.[21,29−34] Up until now, the broad application of UCNPs in microscopy imaging suffers a hindrance resulting from the absence of a commercially available microscope for UCL imaging, although the utility of up-converting phosphors in biodetection have been investigated.[29−32] Recently, Lim et al.[33] have used up-converting phosphors of particle size 50−200 nm to visualize the digestive system of live *C. elegans*. Zhang et al.[34] have reported on the use of polyethyleneimine (PEI)-coated UCNPs (~50 nm) for cell imaging. However, the resolution of their UCL images, which were obtained by using a wide-field imaging approach with a CCD camera, was not excellent. In addition, this kind of modified microscope fails to provide depth discrimination and three-dimensional visualization capability.

In the present study, we have revealed for the first time that the out-of-focus UCL signal of UCNPs greatly obscured the in-focus detail and resulted in the poor image quality. Moreover, we have developed a new method of laser scanning up-conversion luminescence microscopy (LSUCLM) capable of eliminating the interference of the out-of-focus signal and improving the resolution of the UCL images, which was proven as a novel three-dimensional visualization tool with little photobleaching and no background fluorescence. Furthermore, LSUCLM can be readily conducted in conjunction with conventional confocal fluorescence imaging to provide more details about complex biological samples, promising its wide application by more investigators.

EXPERIMENTAL SECTION

Materials. As UCNPs, $NaYF_4$: 20 mol % Yb, 2 mol % Er nanophosphors of diameter ~20 nm were synthesized by a modified hydrothermal route assisted by oleic acid.[29,35] The oleic acid-capped UCNPs were hydrophobic and could be well dispersed in nonpolar solvents (such as cyclohexane or chloroform) (see Figure S1a in the Supporting Information). Subsequently, the oleic acid ligands on the surface of the UCNPs were converted to azelaic acid ($HOOC(CH_2)_7COOH$) ligands by Lemieux−von Rudloff oxidation according to our recently developed method.[29] Under CW excitation at 980 nm (0~600 mW, Connet Fiber Optics, China), both the oleic acid-capped UCNPs in cyclohexane and the azelaic acid-capped UCNPs in water showed intense green (510−560 nm) and red (635−680 nm) emission bands (Figure S2 in the Supporting Information). Organic dyes DiI ($DiIC_{18}(3)$) and DAPI were purchased from Biotium and Beyotime, respectively.

Implementation of LSUCLM. The instrument was built on an inverted microscope (Olympus IX81) and a confocal scanning unit (FV1000, Olympus, Japan). The CW laser emitting at 980 nm was directed by the galvanometer mirrors and then focused by an objective lens into the specimen. Light emitted from the location of the scanning spot was deflected by the galvanometer mirrors and then separated from the excitation by a reverse excitation dichroic mirror (Excitation DM, short-pass, edge at 850 nm, model 850DMSP, OMEGA), then passed through a confocal pinhole and a filter, and finally entered a photomultiplier tube (R6357 Enhanced model, HAMAMATSU, Japan) as a detector.

Imaging Modality Experiment. An aqueous solution of rhodamine B in a quartz cuvette was excited using a two-photon laser scanning microscope (Olympus FV1000, BX61W1, upright position) with a 10× air-immersion objective lens (NA 0.40, Olympus, Japan). Single-photon excitation at 488 nm was provided by a multiline Ar laser. Two-photon excitation through femtosecond pulses at 880 nm was provided by a Ti:sapphire femtosecond laser source (Coherent Chameleon Ultra). The oleic acid-capped UCNPs in cyclohexane were excited from the CW laser or femtosecond pulses at 980 nm.

Pinhole Experiment. Oleic acid-capped UCNPs embedded in a poly(methyl methacrylate) film were imaged on the two-photon microscope with femtosecond pulses at 980 nm. Emission at 500−560 nm was collected from the detection system with a pinhole of the adjustable diameter of 0~800 μm.

Cell Labeling with UCNPs. HeLa cells (Institute of Biochemistry and Cell Biology, China) were incubated with 5 μM DiI in

(16) Billinton, N.; Knight, A. W. *Anal. Biochem.* **2001**, *291*, 175–197.
(17) Troy, T.; Jekic-McMullen, D.; Sambucetti, L.; Rice, B. *Mol. Imaging* **2004**, *3*, 9–23.
(18) Mansfield, J. R.; Gossage, K. W.; Hoyt, C. C.; Levenson, R. M. *J. Biomed. Opt.* **2005**, *10*, 41207.
(19) Auzel, F. *Chem. Rev.* **2004**, *104*, 139–173.
(20) Heer, S.; Kömpe, K.; Güdel, H. U.; Haase, M. *Adv. Mater.* **2004**, *16*, 2102–2105.
(21) Sivakumar, S.; van Veggel, F. C. J. M.; Raudsepp, M. *J. Am. Chem. Soc.* **2005**, *127*, 12464–12465.
(22) Zhang, P.; Rogelj, S.; Nguyen, K.; Wheeler, D. *J. Am. Chem. Soc.* **2006**, *128*, 12410–12411.
(23) Boyer, J. C.; Vetrone, F.; Cuccia, L. A.; Capobianco, J. A. *J. Am. Chem. Soc.* **2006**, *128*, 7444–7445.
(24) Li, Z.; Zhang, Y. *Angew. Chem., Int. Ed.* **2006**, *45*, 7732–7735.
(25) Mai, H. X.; Zhang, Y. W.; Si, R.; Yan, Z. G.; Sun, L. D.; You, L. P.; Yan, C. H. *J. Am. Chem. Soc.* **2006**, *128*, 6426–6436.
(26) Zhang, P.; Steelant, W.; Kumar, M.; Scholfield, M. *J. Am. Chem. Soc.* **2007**, *129*, 4526–4527.
(27) Feng Wang, F.; Liu, X. G. *J. Am. Chem. Soc.* **2008**, *130*, 5642–5643.
(28) Zhou, Z. G.; Hu, H.; Yang, H.; Yi, T.; Huang, K. W.; Yu, M. X.; Li, F. Y.; Huang, C. H. *Chem. Commun.* **2008**, 4786–4788.
(29) Chen, Z. G.; Chen, H. L.; Hu, H.; Yu, M. X.; Li, F. Y.; Zhang, Q.; Zhou, Z. G.; Yi, T.; Huang, C. H. *J. Am. Chem. Soc.* **2008**, *130*, 3023–3029.
(30) Rantanen, T.; Päkkilä, H.; Jämsen, L.; Kuningas, K.; Ukonaho, T.; Lövgren, T.; Soukka, T. *Anal. Chem.* **2007**, *79*, 6312–6318.
(31) Rantanen, T.; Järvenpää, M.-L.; Vuojola, J.; Kuningas, K.; Soukka, T. *Angew. Chem., Int. Ed.* **2008**, *47*, 3811–3813.
(32) van de Rijke, F.; Zijlmans, H.; Li, S.; Vail, T.; Raap, A. K.; Niedbala, R. S.; Tanke, H. J. *Nat. Biotechnol.* **2001**, *19*, 273–276.
(33) Lim, S. F.; Riehn, R.; Ryu, W. S.; Khanarian, N.; Tung, C. K.; Tank, D.; Austin, R. H. *Nano Lett.* **2006**, *6*, 169–174.
(34) Chatterjee, D. K.; Rufaihah, A. J.; Zhang, Y. *Biomaterials* **2008**, *29*, 937–943.
(35) Wang, L. Y.; Li, Y. D. *Chem. Mater.* **2007**, *19*, 727–734.

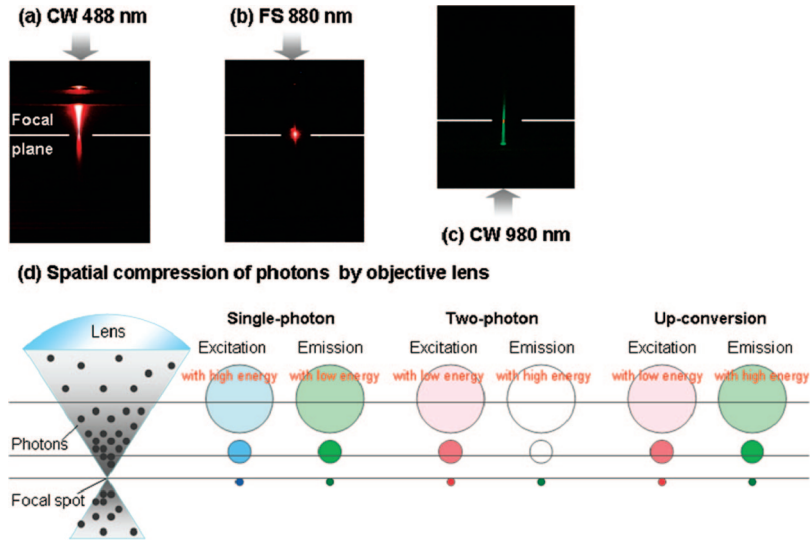

Figure 1. Principles and imaging modalities of single-photon emission, two-photon emission, and up-conversion luminescence (UCL). Photographs illustrate fluorescence in a cuvette of rhodamine B resulting from focused laser beams using single-photon excitation with continuous wave (CW) at 488 nm (a), two-photon excitation with femtosecond pulses (FS) at 880 nm (b), and UCL of UCNPs under CW excitation at 980 nm (c). In particular, the excitation path in panel c goes through the cuvette from the bottom to the top. The spatial compression of photons by the objective lens is shown in part d; the excitation photon density is greatest at the focal spot and rapidly decreases with distance from this region.

Ca/Mg-free PBS for 20 min at 37 °C under 5% CO_2, resulting in the cytoplasm staining. Subsequently, the cells were incubated with 200 μg/mL azelaic acid-capped UCNPs for 2 h. After washing with PBS to remove excess UCNPs, the cells were fixed with 4% paraformaldehyde, and their nuclei were stained with 5 μg/mL DAPI in 10% glycerol. The multilabeled cells were then imaged by LSUCLM in combination with conventional confocal microscopy (Figure S3 in the Supporting Information). The fluorescence signals of DAPI and DiI were measured in the nuclei and cytoplasm, respectively (Figure S4a,b in the Supporting Information).

Photobleaching Experiment. By virtue of a three-channel detection system of LSUCLM (Figure S5 in the Supporting Information), the luminescence signals of DAPI, DiI, and UCNPs could be detected simultaneously under excitation at 405, 543, and 980 nm, respectively. First, photobleaching of the organic dyes was measured under constant illumination by a CW laser at 980 nm with a high power of ~19 mW in the focal plane (obtained by an optical power meter Advantest, TQ8210). Also, 405 and 543 nm lasers with very low power of ~15 and 0.8 μW in the focal plane were used as excitation sources for DAPI and DiI, respectively, to reduce their photobleaching but to ensure the detection of the fluorescence signals of DAPI and DiI. Second, the photostability of the UCNPs was then compared with those of the organic dyes under simultaneous illumination provided by CW lasers at 405, 543, and 980 nm with high powers of approximately 1.6, 0.13, and 19 mW in the focal planes, respectively. To further quantify the rate of photobleaching, the luminescence intensity of each dye was collected from a selected region and was then integrated, normalized, and plotted as a function of time.

Safety Considerations. Because DAPI easily enters live cells and binds tightly to DNA, it is toxic and mutagenic. Care should be taken in its handling and disposal.

RESULTS AND DISCUSSION

The imaging modality of the UCL of the UCNPs was investigated in comparison with those of single-photon and two-photon emission microscopy imaging. As shown in Figure 1, there are clear differences between the single-photon and two-photon emission of rhodamine B (as an example of an organic dye) and the UCL of the UCNPs. (1) In the single-photon emission of rhodamine B, besides the fluorescence from the focal spot, emission was also observed above and below the focal plane (Figure 1a). This out-of-focus fluorescence adversely affects the in-focus image, resulting into poor axial resolution in conversional wide-field imaging. In order to reject the out-of-focus light, confocal microscopy adopts a laser scanning point imaging, by which individual regions are illuminated in sequence and at the same time all but the illuminated regions is masked from light to the detector by a pinhole aperture. (2) In the case of the two-photon excitation of rhodamine B, due to the quadratic relationship between excitation intensity and fluorescence emission,[5,6] light was generated only at the focal point of the focused laser beam (Figure 1b). Therefore, two-photon emission yields intrinsic three-dimensional resolution, and the confocal pinhole may be omitted from the detection system for two-photon imaging. (3) In the case of the UCL of UCNPs, however, luminescence was observed along the path of the laser beam (Figure 1c). Moreover, the relatively low molar absorption coefficient of rare earth ions led to very little attenuation of the beam energy, and hence an extension of the UCL with a symmetrical conical shape was found above and below the focal plane. A similar result was obtained under excitation from femtosecond pulses at 980 nm (Figure S6d in the Supporting Information). This might be attributed to the unique up-conversion mechanism of UCNPs, involving multiple photon absorptions and energy transfers through a series of real levels (Figure S7), which was in agreement with the observation of the nonlinear dependence between the excitation power and up-conversion lumines-

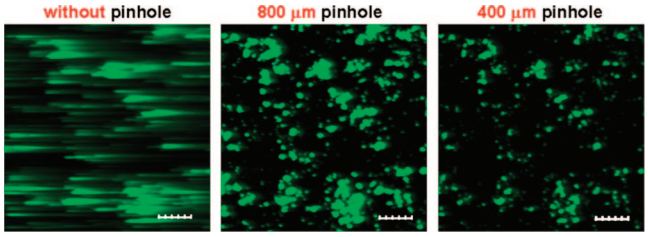

Figure 2. UCL images of a poly(methyl methacrylate) film containing embedded UCNPs obtained using a two-photon laser scanning microscope in the absence or presence of a pinhole (λ_{ex} = 980 nm; femtosecond pulses; emission was collected at 500−560 nm; scale bar, 50 μm).

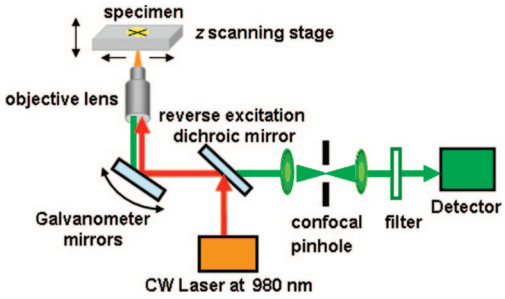

Figure 3. Schematic layout of a laser scanning up-conversion luminescence microscopy (LSUCLM) system setup. The excitation laser beam path is shown in red, and the emission pathway is shown in green (for details see Experimental Section).

cence of UCNPs (Figure S2b in the Supporting Information).[19] These results indicate that the emission modality of UCL is significantly distinct from those of two-photon and single-photon emission (Figure 1d) and that the out-of-focus UCL becomes a significant hindrance to the utility of UCNPs in bioimaging.

In view of the successful use of the confocal pinhole to improve axial resolution in confocal microscopy, herein, a pinhole was adopted in the present UCL imaging to reject out-of-focus light. To further explore the effect of the pinhole on the quality of the UCL image, imaging of UCNPs was carried out in the presence and absence of a pinhole. As shown in Figure 2, a detection system without a pinhole yielded a poor UCL image. Besides the axial interference from out-of-focus light, lateral (or in-plane) interference from scattering within the focal plane also completely obscured the in-focus detail. With the use of a pinhole of 800 μm diameter, however, the axial and lateral interference was greatly suppressed and an image with slightly protracted signals was obtained. Upon further reduction of the diameter of the pinhole to 400 μm, a high-quality UCL image appeared. These results demonstrated that the influence of the out-of-focus UCL could be largely eliminated by introducing the confocal pinhole, and the adverse effect of scattering within the focal plane was also avoided.

The application of UCNPs in microscopic imaging demands the development of a novel microscopy technique, namely, laser scanning up-conversion luminescence microscopy (Figure 3). Because of the "optical sectioning" effect provided by the confocal pinhole, LSUCLM allows the construction of three-dimensional (3D) UCL images. This 3D visualization capability was illustrated by serially scanning a poly(methyl methacrylate) film containing embedded UCNPs at increasing depths along the *z*-axis. Figure

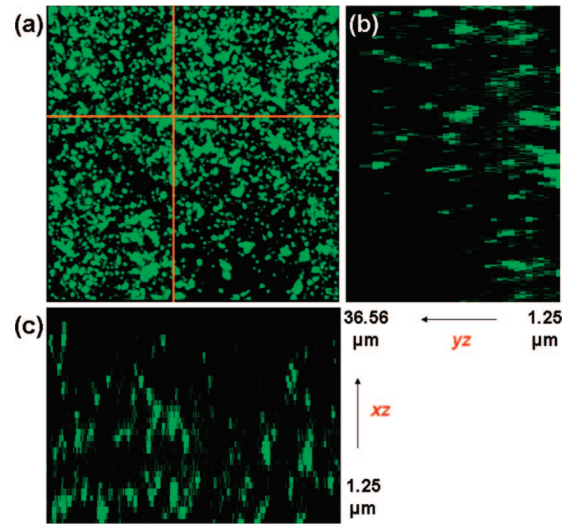

Figure 4. Three-dimensional UCL images of a poly(methyl methacrylate) film containing embedded UCNPs performed by LSUCLM. (a) Two-dimensional projection image of 34 depth-resolved slices separated by 1.07 μm. Parts b and c display the *yz* and *xz* cross sections taken at the lines shown in panel a, respectively (λ_{ex} = 980 nm; continuous wave; the power in the focal planes of ~19 mW; emission was collected at 500−560 nm; image size, 800 × 800 pixel; sampling speed, 10.0 μs/pixel; pinhole, 123 μm, 60× oil-immersion objective lens; NA 1.35; zoom, ×4.0).

4a displays a two-dimensional overlap that is composed of 34 depth-resolved slices separated by 1.07 μm. Importantly, the UCNPs are clearly visible in the *yz* and *xz* cross-sectional UCL images at different depths (1.25−36.56 μm) (Figures 4b,c and Movie 1 in the Supporting Information).

Further practical application of LSUCLM in the visualization of biological samples demonstrated that HeLa cells could be labeled with UCNPs by a noninvasive technique based on the ability of cells to endocytose. Intense luminescence signals at 500−560 nm were detected from the cells (Figure S4c in the Supporting Information), when excitation was provided by a CW laser at 980 nm. A spectrum scan experiment revealed that the luminescence exhibited two emission bands with maxima at 545 and 660 nm, respectively (Figure S8 in the Supporting Information), confirming that the luminescence was originated from the UCNPs. As shown by the overlay of DAPI, DiI, and UCNPs images (Figure S4e in the Supporting Information), the UCL signal was seen to be colocalized with the fluorescence of DiI but excluded from the regions stained with DAPI, suggesting that the UCNPs were internalized by the cells but could not enter the nuclei. In a control experiment, a very weak UCL signal was measured when the cells were incubated with 200 μg/mL of azelaic acid-capped UCNPs for 2 h at 4 °C (Figure S9 in the Supporting Information). These observations implied that the UCNPs had been transported into the cells by endocytosis, because the materials entering cells via an active transport mechanism can be blocked at 4 °C. Such an internalization of UCNPs by HeLa cells was further supported by TEM. In an electron micrograph of the cells, a large number of UCNPs were observed in the vesicles, which resided in the cytoplasm (Figure S10 in the Supporting Information). These results establish that HeLa cells may be labeled with UCNPs by a noninvasive technique based on the ability of cells to endocytose.

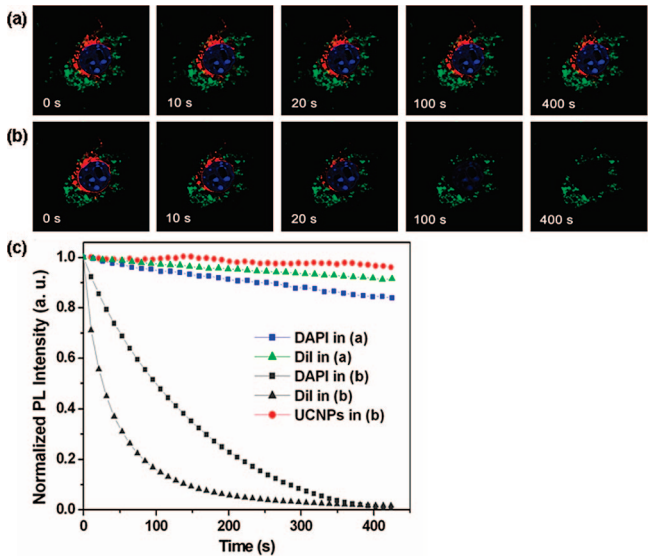

Figure 5. Comparison of photobleaching in LSUCLM and conversional confocal microscopy imaging. The luminescence signals of DAPI and DiI are shown in blue and red, respectively, and that of UCNPs is displayed in green in the pseudocolor image. (a) Excitation was provided by a CW laser at 980 nm at a high power (~19 mW in the focal plane), whereas the excitations at 405 and 543 nm were controlled at a very low power (~15 and 0.8 μW in the focal plane for 405 and 543 nm, respectively). (b) Simultaneous excitations was provided by CW lasers at 405, 543, and 980 nm with powers of approximately 1.6, 0.13, and 19 mW in the focal plane, respectively. (c) Quantitative analysis of the changes in fluorescence intensities of DAPI, DiI, and UCNPs in panels a and b.

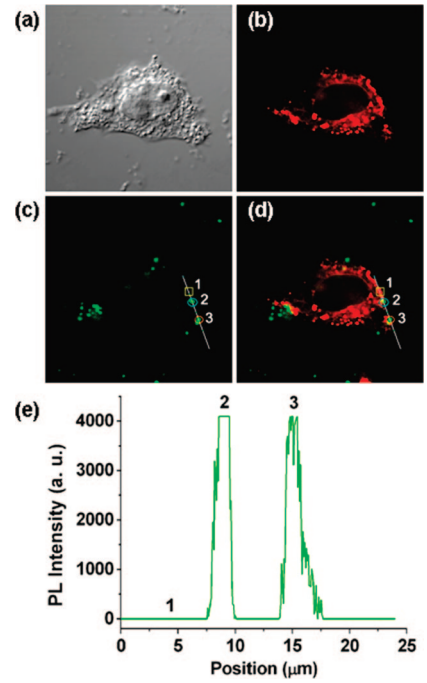

Figure 6. Images of a live HeLa cell dual-labeled with DiI and UCNPs. (a) Differential interference contrast brightfield image. (b) Image of DiI when emission was collected at 560−600 nm (λ_{ex} = 543 nm). (c) UCL image of UCNPs when emission was collected at 500−600 nm (λ_{ex} = 980 nm). The overlay of panels b and c is shown in panel d. (e) UCL intensity profile along the lines shown in panels c and d (the output power of the laser was 400 mW, corresponding to approximately 19 mW in the focal planes; image size, 800 × 800 pixel; sampling speed, 2.0 μs/pixel; pinhole, 197 μm; 60× oil-immersion objective lens; NA 1.35; zoom, ×3.5).

Subsequently, the degree of photobleaching in LSUCLM was compared with that in conventional confocal microscopy by means of time-sequential scanning of a multilabeled cell. First, after 425 s of illumination by a CW laser at 980 nm with a high power, DAPI and DiI still retained 84% and 90% of their initial intensities, respectively (Figure 5a,c and Figure S12 and Movie 2 in the Supporting Information). In a control experiment without 980 nm illumination, the signals of DAPI and DiI were 94% and 99% of their initial values, respectively (Figure S13 in the Supporting Information). That is, very weak photobleaching of DAPI or DiI was induced by long-term exposure to the high-power CW laser at 980 nm. Second, under the simultaneous and high-power illumination provided by CW lasers at 405, 543, and 980 nm for 400 s, the UCL intensity of UCNPs still remained at 96% of its initial value at the end of the illumination (Figure 5b, 5c and Figure S14 and Movie 3 in the Supporting Information), whereas the fluorescence intensity of DiI and DAPI decreased rapidly to 2.5% and 1% of their initial values. These data showed the first quantitative measurement of photobleaching of UCNPs and organic dyes under CW 980 nm illumination with superhigh power density of ~4.6×10^6 W cm^{-2}. Moreover, in view of the facts that continuous illumination by CW laser light at 980 nm induces little photobleaching of UCNPs and the colabeled fluorophores, we can deduce that LSUCLM provides a visualization tool with little photobleaching that far surpasses conventional confocal imaging in this respect.

Furthermore, to determine the signal sensitivity of LSUCLM imaging, live HeLa cells were labeled with DiI and low-concentration azelaic acid-capped UCNPs (50 μg/mL) (Figure 6). It is worthy to note that no signal from DiI or autofluorescence was obtained in the UCL image of a cell (Figure 6c), even though a broad detection channel for the UCNPs (500−600 nm) was deliberately chosen to overlap with that of DiI (560−600 nm). The lack of autofluorescence resulting from 980 nm excitation has been pointed out in previous reports.[19,29−32,34] Up until now, however, no quantitative data on the signal-to-noise ratio of UCL imaging is obtained by experiments. Herein, as shown in Figure 6e, quantization of the UCL profile across the line shown in Figure 6c,d reveals an excellent signal-to-noise ratio with extremely high UCL signals (counts >4095, regions 2 and 3) and no background fluorescence (counts ~0, region 1 containing the DiI-stained region). This is the first quantitative data for the lack of autofluorescence under 980 nm excitation. Such a superhigh signal-to-noise ratio may be attributed to two factors, the first being the very weak single-photon absorption of conventional luminescent materials at 980 nm, and the second being the very low likelihood of them absorbing two photons simultaneously under CW excitation at 980 nm. Thus, we can conclude that LSUCLM imaging using UCNPs as labels is capable of completely eliminating background fluorescence from either endogenous fluorophores or colabeled fluorescent probes and hence produces extremely high sensitivity and specificity for the imaging of biological specimens.

CONCLUSIONS

In summary, we have revealed that the out-of-focus UCL signal can greatly obscure the in-focus detail, resulting in poor image

quality. By introducing the pinhole technique, we successfully eliminated the interference of out-of-focus UCL and thereby developed a three-dimensional visualization tool, laser scanning up-conversion luminescence microscopy. Compared with conventional single-photon and two-photon fluorescence imaging techniques, LSUCLM in combination with up-conversion luminescent labels under a CW 980 nm excitation has some distinct advantages: (1) the low level of photobleaching of both organic dyes and UCNPs promise its utility in long-term imaging; (2) the complete elimination of background interference from either endogenous fluorophores or colabeled fluorescent probes provides an extremely high sensitivity; and (3) the convenience and low cost of the CW near-infrared laser can be expected to enable wide application by more investigators. Furthermore, LSUCLM imaging of UCNPs may be readily conducted in conjunction with conventional confocal imaging to provide more details about complex biological samples. Thus, all of these advantages of LSUCLM imaging method promise wide application in chemistry, biological, as well as materials sciences.

ACKNOWLEDGMENT

The authors are thankful for the financial support from NSFC (Grants 20825101 and 20775017), NHTPC (Grant 2006AA03Z318), Grant NCET-06-0353, Shanghai Science and Technology Community (Grant 06QH14002), and the Shanghai Leading Academic Discipline Project (Grant B108).

SUPPORTING INFORMATION AVAILABLE

Additional information as noted in text. This material is available free of charge via the Internet at http://pubs.acs.org.

Received for review July 11, 2008. Accepted December 11, 2008.

AC802072D